Металлофиз. новейшие технол. / Metallofiz. Noveishie Tekhnol.
2015, т. 37, № 5, сс. 593–604
Оттиски доступны непосредственно от издателя
Фотокопирование разрешено только
в соответствии с лицензией

PACS numbers: 71.15.Ap, 71.15.Mb, 71.15.Nc, 71.20.Eh, 71.70.Gm, 75.50.Ee, 88.30.rd

Electronic Structure of the Rare-Earth Dihydride GdH_2

Z. Ayat, B. Daoudi, A. Ouahab*, and A. Boukraa

Université Ouargla,
Faculté des Mathématiques et des Sciences de la Matière,
Laboratoire Développement des Energies Nouvelles et Renouvelables
dans les Zones Arides et Sahariennes,
30000 Ouargla, Algeria
**Université Mohamed Khider,*
Département des Sciences de la Matière,
Faculté des Sciences Exactes et des Sciences de la Nature et de la Vie,
07000 Biskra, Algeria

With the WIEN2k simulation code, the *ab initio* calculations of electronic properties for the cubic stoichiometric rare-earth dihydride GdH_2 (in the cubic fluorite structure) are performed using the full-potential linearized augmented plane wave (FP-LAPW) method approach within the density functional theory (DFT) in the generalized gradient approximation (GGA) (used for the exchange–correlation potential). The lattice parameter, the bulk modulus, its pressure derivative, the density of states, and the energy band structures are determined. Two low-lying hydrogen–metal bands of GdH_2 are observed. The Fermi energy E_F falls at a level where most of the states are rare-earth 5*d* conduction states. Information on the negligible role of the H1*s* state contribution near E_F is obtained.

З використанням пакету для моделювання WIEN2k виконано *ab initio* розрахунки електронних властивостей для кубічного стехіометричного рідкісноземельного дигідриду GdH_2 (в структурі кубічного флюориту) із застосуванням повнопотенціяльної методи лінеаризованих приєднаних пласких хвиль в межах теорії функціоналу густини в наближенні узагальненого ґрадієнту (застосованих до обмінно-кореляційного потенціялу). Визначено сталу кристалічної ґратниці, модуль об'ємної пружности, його похідну за тиском, густину станів та структури енергетичних зон. Енергія Фермі E_F розташовується поблизу рівня, де більшість станів є провідними 5*d*-станами рідкісноземельного елементу. Одержано інформацію щодо нехтовно малої ролі внеску стану H1*s* поблизу E_F.

С использованием пакета для моделирования WIEN2k проведены *ab initio*

расчёты электронных свойств для кубического стехиометрического редкоземельного дигидрида GdH_2 (в структуре кубического флюорита) с применением полнопотенциального метода линеаризованных присоединённых плоских волн в рамках теории функционала плотности в приближении обобщённого градиента (применённых к обменно-корреляционному потенциалу). Определены постоянная кристаллической решётки, модуль объёмной упругости, его производная по давлению, плотность состояний и структуры энергетических зон. Энергия Ферми E_F располагается вблизи уровня, где большинство состояний являются проводящими 5d-состояниями редкоземельного элемента. Получена информация о пренебрежимо малой роли вклада состояния H1s вблизи E_F.

Key words: rare-earth dihydrides, GdH_2, density functional theory, *ab initio* calculations, WIEN2k.

(Received January 8, 2015)

1. INTRODUCTION

Hydrogen is considered as an ideal fuel for many types of energy converters. However, the reversible storage of hydrogen in the form of metallic and intermetallic hydrides has several advantages over storings of gaseous and liquid hydrogen. Over the past few decades, a major challenge, which still remains, is to identify optimal candidates in intermetallics for such hydrogen storage. Rare earth (R) alloys are seen as promising materials, owing to high hydrogen capacity per volume unit and an ability to absorb hydrogen under moderate conditions of temperature and pressure [1], where the interstitial hydrogen atoms strongly modify the electronic structure and add interesting features [2].

The rare earth–hydrogen (R–H) phase diagram as presented in Fig. 1 is characterized by broad existence ranges around the stoichiometric compositions: the h.c.p. α-phase solid solution of the parent metal, the cubic β-phase dihydrides and h.c.p. γ-phase trihydrides [3].

Dihydrides are obtained from an exothermic reaction, which forms stable compounds crystallizing in the cubic fluorite structure of the CaF_2 type [4]. This crystal structure consists of two sublattices: the f.c.c. sublattice of the R-atoms, and that of the H atoms occupying ideally all the tetrahedral interstices of the former (Fig. 2 is obtained by using visualisation program XCrySDen [5]). More than 30 years ago, the electronic structure of rare earth (including scandium and yttrium) dihydrides was investigated by photoemission [6], where the effects of hydrogenation on the density of states were investigated. These experiments were later combined with theoretical calculations to establish the quasi-anionic (or 'hydridic') nature of hydrogen atoms [7, 8].

Because of the similarity in the electronic structure of rare earths, and in order to simplify as much as possible the role of f-electrons, we

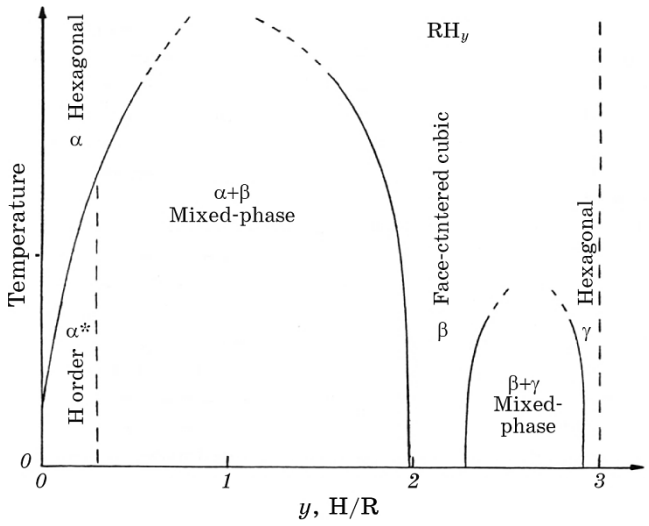

Fig. 1. Typical phase diagram of R–H systems.

have concentrated on GdH_2.

The low-temperature magnetic ordering of the nonstoichiometric compounds GdD_{2+x} for $|x| < 0.20$ has been investigated by neutron diffraction and magnetic susceptibility measurements. The magnetic structure of $GdD_{1.93}$ is antiferromagnetic of MnO type, with a propagation vector $\tau = (1/2)[111]$, whereas a helical structure with axis along the <111> direction is observed for GdD_2. The angle between the moments in the successive (111) layers is 163.8°, the T_N, which was 20 K for $GdD_{1.93}$, decreases regularly to $T_N = 15.5$ K for $GdD_{2.00}$ [9].

The magnetic structure of pure GdH_2 is AF of MnO type below T_N, with a propagation vector $\zeta_n = (1/2)[111]$ [10]. The problem of the sometimes strong variation between the magnetic parameters of $GdH_{2\pm x}$ (and other R systems) from various sources is related to a lack-

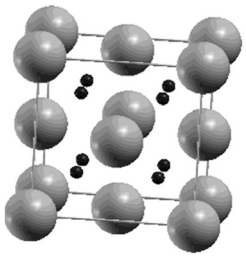

Fig. 2. The compound crystallises in the CaF_2 fluorite type structure: the large spheres represent rare earth atoms (×4) and small spheres hydrogen atoms occupying tetrahedral sites (×8) (figure plotted with XCrySDen [3]).

ing definition of the 'pure' dihydride $RH_{2.00}$ and has been discussed for example by Vajda (1995) [4].

In this paper, we will focus our attention on the electronic properties of GdH_2 through a first-principles calculation at 0 K, without considering its magnetic aspect. The calculation is based on density functional theory employing the full-potential linear augmented plane wave (FP-LAPW) method. A good review of *ab initio* methods as applied to fluorite-type R hydrides is given in the first chapter of a recent publication by Schöllhammer (2013) [12]. A compilation of physical properties of R (and actinide) dihydrides is presented in the second chapter of the same book by Vajda (2013) [13].

The rest of this paper is organized as follows: in Section 2 the calculation method is described. Section 3 gives the results of the calculations and discussion. Finally, Section 4 concludes the paper.

2. COMPUTATIONAL METHOD

Our calculations are based on density functional theory (DFT) [13, 14]. In this work, the full-potential linearized augmented plane wave (FP-LAPW) method as implemented in the WIEN2k package [15] is used for the calculations. The Kohn–Sham equations are solved self-consistently using FP-LAPW. In this method, electronic wave functions, the charge density, and the crystal potential are expanded as spherical harmonics inside the non-overlapping atomic spheres of radius R_{MT}, and as plane waves in the remaining space of the unit cell. The muffin-tin radii (the atomic spheres radii), R_{MT}, selected for Gd and H were 2.25 and 1.8 Bohr radius, respectively. We have chosen the basis set size $R_{MT}^{min} K_{max} = 9$, where R_{MT}^{min} is the smallest atomic sphere radius inside the cell, and K_{max} is a cut-off for the basis function wave vector. The cut-off in the charge density Fourier expansion, G_{max}, is taken to be 20 $Ry^{1/2}$. We also mention that the integrations over the Brillouin zone are performed up to 400 **k**-points in its irreducible wedge. We used an energy to separate core and valence states equal to –8 Ry. Exchange and correlation effects are treated within the density functional with the generalized-gradient approximation of Perdew, Burke, and Ernzerhof (GGA96) [16]. We have taken a value of 5.3022 Å [17] as the actual lattice constant for the calculations. The self-consistent calculations are considered to be converged only when the calculated energy changes by less than 0.1 mRy.

3. RESULTS AND DISCUSSION

The ground-state structural parameters have been obtained by minimizing the total energy with respect to the volume by varying the latter in steps of 2% within ±12% from the optimizing value. By fitting

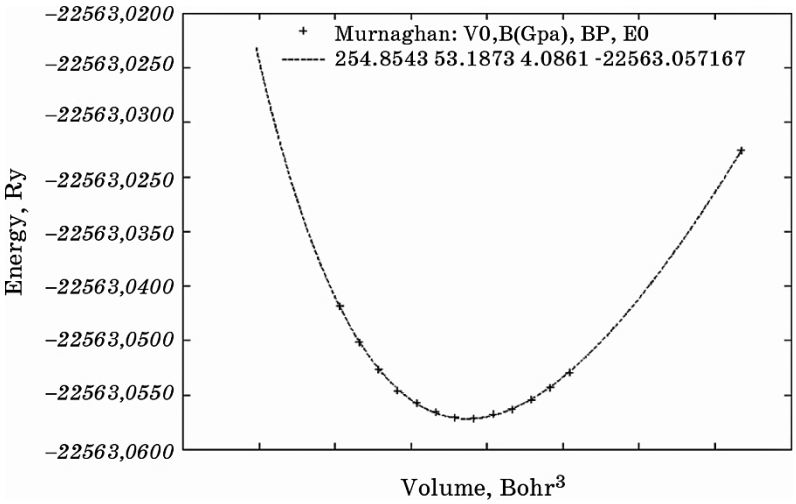

Fig. 3. Total energy of GdH_2 as a function of volume.

this total energy versus volume data to the non-linear Murnaghan equation of state [19] as shown in Fig. 3, we obtained the equilibrium lattice constant, the value of the bulk modulus, and its pressure derivative.

The results are given in Table 1 along with earlier experimental and theoretical findings. Our calculated structural parameters show very good agreement with the theoretical [19, 21] and experimental data [17, 20].

The calculated band structure and total DOS of GdH_2 are shown in Fig. 4, the dashed line indicating the Fermi level. Note that all the 7*f*-

TABLE 1. Equilibrium lattice constant a_0, bulk modulus B_0 (in GPa), pressure derivative B_0', and total energy compared to experimental data and other works: [a]—experiment at 298 K [17], [b]—[19], [c]—our results, [d]—[20], [e]—[21].

	Equilibrium lattice constant, Å	B_0, GPa	B_0'	Total energy, Ry
Present work	5.326[c]	53.1873[c]	4.0861[c]	−22563.0572[c]
Experiment (at 298 K)	5.296 (extrapolated to 0 K)[a]			
Experiment	5.303[d]			
GGA–Pseudopotential (CASTEP) (Antiferromagnetic)	5.339[e]	77[e]	3.61[e]	
Experiment and spin polarized DFT	5.30[b]			

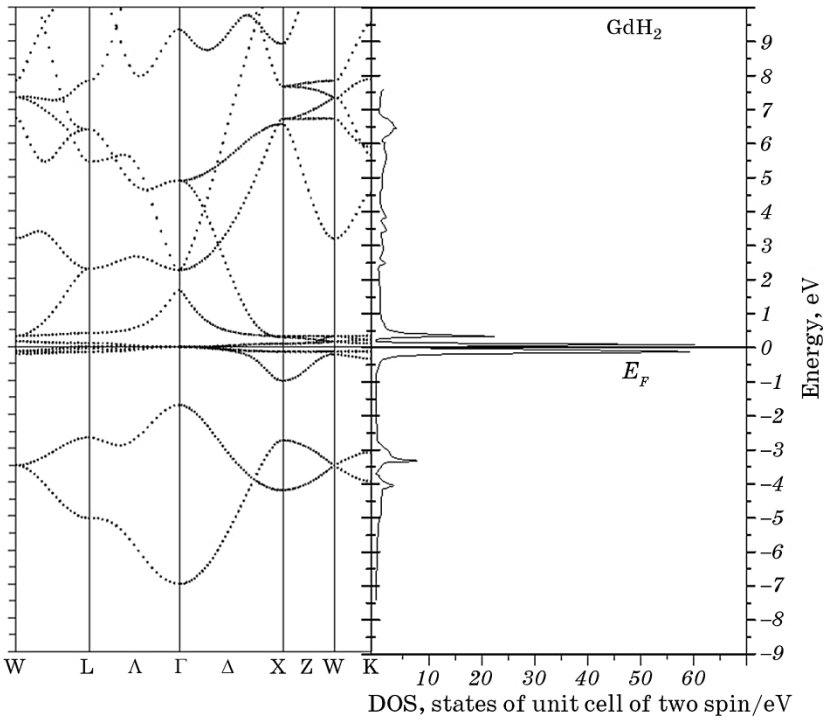

Fig. 4. Density of states (right panel) and electronic band structure along high-symmetry directions (left panel) of GdH_2, the Fermi energy being at 0 eV.

electrons are found in a single unsplit peak at E_F thus missing the strong correlation between *f*-electrons. This is not acceptable from the point of view of the electronic distribution. In order to circumvent this problem, DFT calculations going beyond the LDA/GGA scheme level can improve to some extent on the treatment of correlation: methods such as LDA + U, self-interaction correction (SIC) and open core calculations have been cited [22].

In this work, we used the less sophisticated 'open core' approach in which contributions of the 4*f*-electrons are removed from the valence bands, a procedure equivalent to the LDA + U approximation, where $U = +\infty$ for the *f*-electrons.

These *f*-electrons are treated as atomic electrons, *i.e.* they cannot hybridize with the other valence *s*-, *p*-, and *d*-electrons anymore and are perfectly localized [23].

However, one can expect the existence of finite localized magnetic moments on the 4*f*-electrons. This magnetic aspect has not been considered in our calculations.

After applying the open core procedure, the calculation is iterated until convergence. This establishes the values of the Fermi energy E_F

TABLE 2. Fermi energy and density of states at the Fermi level for GdH_2.

	Fermi energy, eV	$N(E_F)$, states unit cell of two spins/Ry
GdH_2	7.0981	13.3759

and the density of states at the Fermi level $N(E_F)$ (Table 2).

The band structure and total density of states calculated using the 'open core' treatment of GdH_2 is shown in Fig. 5. The unit of density of states is in a state of unit cell of 2 spins/eV and the energy is the electron volt. The energy origin in this figure indicates the Fermi level.

Note that the only difference with the previous calculations is the shifting of the sharp peak due to 4*f*-electrons above the Fermi energy.

We calculated the electronic band structures at the equilibrium lattice constant for different high-symmetry points in the Brillouin zone.

Figure 5 shows qualitative agreement with calculations made by Gupta (1980) [1], Switendick (1971) [8], Misemer *et al.* (1982) [9] on rare-earth systems and a good agreement with the photoemission experiments by Koitzsch *et al.* (2004) [20] on this particular GdH_2 sys-

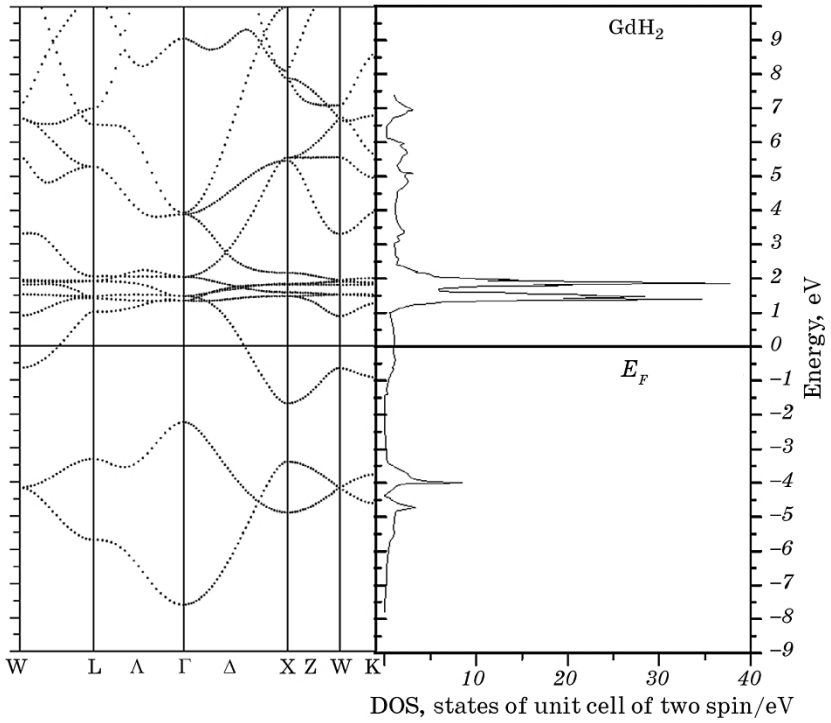

Fig. 5. Density of states (right panel) and electronic band structure along high-symmetry directions (left panel) of GdH_2, the Fermi energy being at 0 eV.

tem, and particularly with those of Fujimori *et al.* (1982) [25]. This figure indicates that only two new bands are added below the Fermi energy and above $E = -7.6417$ eV, along with the two electrons. The new bands are direct consequence of there being two hydrogens in the unit cell and would not appear in structures with only one hydrogen in the unit cell, although the presence of the two low-lying metal–hydrogen bands is a feature common to all the fluorite-structure metal dihydrides [25]. These low-lying bands play an important role in the stability of the compound as was confirmed by UV-photoemission experiments by Weaver *et al.* [6]. The width of the valence band is 5.3607 eV, which is much smaller than that of TiH_2; this is caused by the small H–H separation leading to the large H–H interaction in TiH_2. This confirms that the valence bandwidth is principally determined by the H–H interaction and therefore sensitive to the H–H distance [25].

In order to analyse the atomic interaction between a hydrogen atom and its different neighbouring atoms, the total DOS has been decomposed into its partial-wave (*s*-, *p*-, *d*- and *f*-) components around the H where each Gd site sits in the middle of a cube with eight tetrahedral sites at the corners.

In Figures 6 and 7, we show the total DOS decomposition into components according to the value of the angular momentum (s: $L = 0$; p: $L = 1$; d: $L = 2$; f: $L = 3$) inside the MT spheres of the metal and of the hydrogen. One can clearly see that the two low-lying bands are largely formed by the *s*-states of hydrogen. Indeed, the shape of the $L = 0$ component of the DOS inside the hydrogen MT spheres has a structure of two peaks, and this shape is very similar to the total DOS. Cubic symmetry leads to the degeneration of states of metallic quintuple states in triple (d-t_{2g}) and double (d-e_g) states [1]. Some d-t_{2g}-states, and, to a lesser extent, *s*- and *p*-states of the metal have been significantly affected by the interaction of metal–hydrogen (Me–H) (orbits of the hydrogen 1*s*), and are located at lower energies (the lowest point at Γ), where the formation of this band poses the question of this bond ionicity; a charge-transfer analysis points to an effective charge transfer away from the metal site to the tetrahedral hydrogen sites [8].

As noted above, it was shown that the hybridization is important in the low-lying bands, which contain a contribution from the metal in addition to that of hydrogen (Fig. 8). Dihydrides cannot literally be considered purely ionic compounds [1], even though the results show that hydrogen in tetrahedral sites is negatively charged [4]. The nature of bonding in this compound (and nearly all rare earth dihydrides) must be discussed in terms of interaction between metal *d*-states and hydrogen 1*s*-states [7].

The second electronic band (at Γ and below the *d*-bands) is formed by a combination of antibonding orbitals of the two states of the hydrogen 1*s*-states in the unit cell.

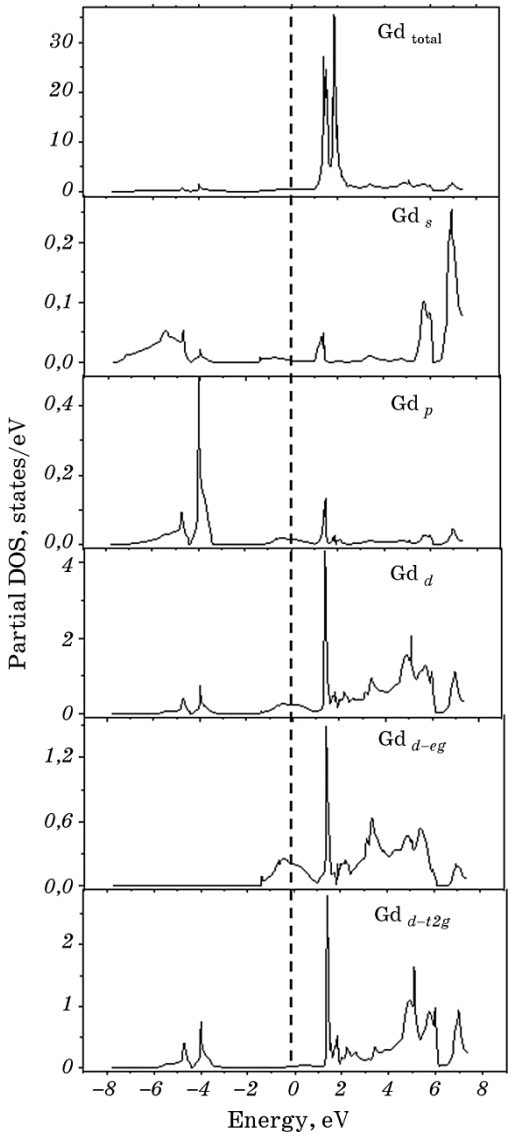

Fig. 6. Orbital-projected DOSs for Gd.

Figure 6 shows the presence of *s* states of the metal on the negative energy side ($E < E_F$) of the first two bands, while the metal *p*-states give an important contribution to the second peak observed below E_F in the total DOS.

On the other hand, the bottom of the conduction band is d-e_g like; we can see that a moderate contribution of Gd*p*-states is present, against a very small contribution from Gd*s*-states and H*s*-states near the Fermi

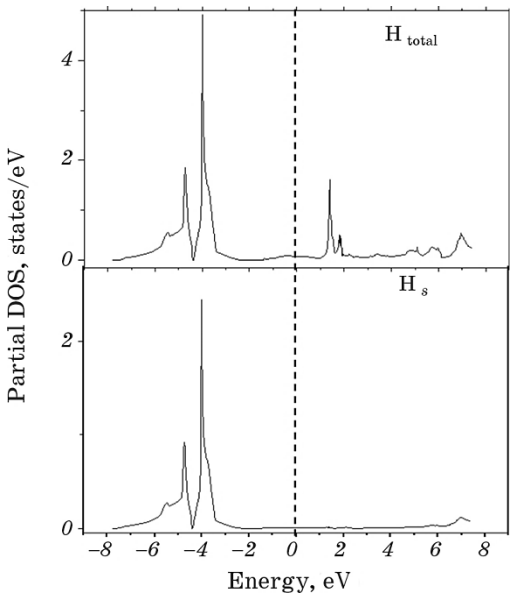

Fig. 7. Orbital-projected DOSs for H_2.

level.

An unoccupied 4*f*-electrons peak is localized in the region of the conduction band some electrons volts above the Fermi level (E_F). This is an artefact due to the 'open core' method used to make the calculation since it is known that the 4*f*-electrons are located in the core of atoms and their states should not appear.

In Figure 5, two large peaks are found in the DOS of the first two bands, with the first peak centred at $E = -4.7301$ eV and the second higher peak at $E = -3.9953$ eV.

These low-lying bands are filled by four of the five valence electrons of this compound, the fifth valence electron filling the bottom of the metal 5*d*-band [1, 7, 8, 24]. In the same figure (band structure), more bands cross $E = E_F$, and therefore, this compound must show a metallic behaviour. This is confirmed by all the profiles of the DOS, which show a finite number of electrons at the Fermi level. The latter lies by 1.383 eV above the bottom of the 5*d*-metal bands.

Net depopulation of the metal 5*d*-bands during hydrogenation, which is a common feature to most rare earth dihydrides, plays an important role in the magnetic properties of these compounds.

4. CONCLUSION

The work presented in this paper was aimed at establishing a clearer

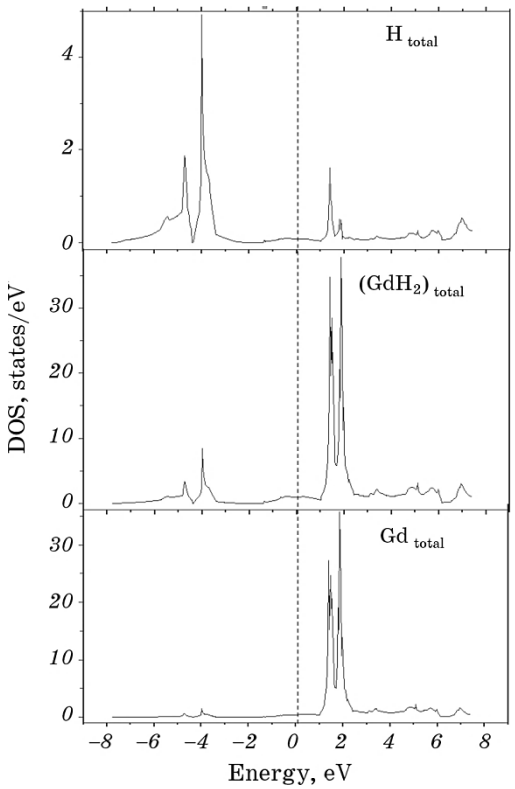

Fig. 8. The calculated total and partial density of states for GdH_2.

picture of the electronic structure for a stoichiometric dihydride, *viz.* β-GdH_2. Calculations performed using an *ab initio* FP-LAPW method as implemented in the WIEN2k code have led to the following conclusions.

The nature of bonding in this compound (and nearly all rare-earth dihydrides) must be discussed in terms of interaction between metal *d*-states and hydrogen 1*s*-states. The position and width of the low-lying bands depend quite sensitively on the type of rare earth considered.

The low-lying bands found in these dihydrides are not composed uniquely of hydrogen *s* states but rather show a strong hybridization with metal *d*- and also metal *s*- and *p*-states.

The Fermi energy E_F falls at a level, where the most of the electronic states are rare-earth 5*d* conduction states.

The H*s*-state has no contribution near the Fermi level.

The lattice constant and the energy band structure are in good agreement with those of Vajda (1995) [4] and Koitzsch *et al.* (2004) [20], respectively.

Generally, we note a good qualitative agreement of our data with

published results on other rare-earth dihydrides.

REFERENCES

1. M. Gupta and J. P. Burger, *Phys. Rev. B*, **22**: 6074 (1980).
2. Y. Fukai, *The Metal–Hydrogen System* (New York: Springer-Verlag: 1993).
3. A. Kokalj, *Comp. Mater. Sci.*, **28**: 155 (2003). Code available from http://www.xcrysden.org.
4. P. Vajda, *Handbook on the Physics and Chemistry of Rare Earths* (Eds. K. A. Gschneidner, Jr. and L. Eyring), vol. **20**, ch. 137, p. 207 (1995).
5. M. Gupta, *Solid State Commun.*, **27**: 1355 (1978).
6. J. Weaver, D. Peterson, and R. Benbow, *Phys. Rev. B*, **20**: 5301 (1979).
7. L. Schlapbach, J. Osterwalder, and H. Siegmann, *J. Less-Common Met.*, **88**: 291 (1982).
8. A. C. Switendick, *Int. J. Quantum Chem.*, **5**: 459 (1971).
9. D. K. Misemer and B. N Harmon, *Phys. Rev. B*, **26**: 5634 (1982).
10. R. R. Arons and J. Schweizer, *J. Appl. Phys.*, **52**: 2645 (1982).
11. P. Vajda, J. N. Daou, and J. P. Burger, *J. Less-Common Met.*, **172–174**: 271 (1991).
12. G. Schöllhammer, F. Karsai, and P. Herzig, *Properties of Fluorite Structure Materials* (Eds. P. Vajda and J.-M. Costantini) (Hauppauge, NY, U.S.A.: Nova Science Pub., Inc.: 2013), ch. 1, p. 1.
13. P. Vajda, *Properties of Fluorite Structure Materials* (Eds. P. Vajda and J.-M. Costantini) (Hauppauge, NY, U.S.A.: Nova Science Pub., Inc.: 2013), ch. 2, p. 31.
14. P. Hohenberg and W. Kohn, *Phys. Rev. B*, **136**: 864 (1964).
15. W. Kohn and L. J. Sham, *Phys. Rev. A*, **140**: 1131 (1965).
16. P. Blaha, K. Schwarz, G. Madsen, D. Kvasnicka, and J. Luitz, *Wien2k, an Augmented Plane Wave Plus Local Orbitals Program for Calculating Crystal Properties* (Vienna: Techn. Universität: 2001).
17. J. P. Perdew, S. Burke, and M. Ernzerhof, *Phys. Rev. Lett.*, **77**: 3865 (1996).
18. M. Chiheb, J. N. Daou, and P. Vajda, *Z. Phys. Chem.*, **179**: 271 (1993).
19. F. D. Murnaghan, *Proc. Nat. Acad. Sci. USA*, **30**: 244 (1944).
20. C. Koitzsch, J. Hayoz, M. Bovet, F. Clerc, L. Despont, C. Ambrosch-Draxl, and P. Aebi, *Phys. Rev. B*, **70**: 165114 (2004).
21. M. Ellner, H. Reule, and E. J. Mittemeijer, *J. of Alloys and Compounds*, **279**: 179 (1998).
22. B. Kong, L. Zhang, X.-R. Chen, M.-S. Deng, L.-C. Cai, and R.-F. Ling-Hu, *J. of Physics and Chemistry of Solids*, **74**: 1322 (2013).
23. S. Jalali Asadabad, S. Cottenier, H. Akbarzadeh, R. Saki, and M. Rots, *Phys. Rev. B*, **66**: 195103 (2002).
24. P. Vajeeston, R. Vidya, P. Ravindran, H. Fjellveg, A. Kjekshus, and A. Skjecltorp, *Phys. Rev. B*, **65**: 075101 (2003).
25. A. Fujimori and N. Tsuda, *Solid State Commun.*, **41**: 491 (1982).
26. A. C. Switendick, *Solid State Commun.*, **8**: 1463 (1970).
27. J. H. Weaver, *Bull. Amer. Phys. Soc.*, **23**: 295 (1978).